Transition from Rain-fed to Irrigation-fed Agriculture in Rural Areas to Exacerbate Urban Water Scarcity

Lokendra S Rathore[1], Mukesh Kumar[1], Naota Hanasaki[2], Mesfin M Mekonnen[1], Pushpendra Raghav[1]

[1] Civil, Construction and Environmental Engineering, The University of Alabama, United States

[2] National Institute for Environmental Studies, Ibaraki, Japan

Corresponding author: Mukesh Kumar (mkumar4@eng.ua.edu)

Key Points:

- Transitioning rainfed agriculture to irrigation-fed increases water scarcity in urban areas.
- The impact magnitude depends on local demand, upstream flow changes due to irrigation expansion, and ancillary sources' buffering capacity.
- Irrigation expansion decisions should consider the impact on water availability both locally and in distant areas to avoid water conflicts.

Abstract

Irrigation expansion is often posed as a promising option to enhance food security. Here, we assess the influence of expansion of irrigation, primarily in rural areas of the contiguous United States (CONUS), on the intensification and spatial proliferation of surface freshwater scarcity. Our study shows that the rainfed to irrigation-fed (RFtoIF) transition of water-scarce croplands can impact scarcity in both transitioned and non-transitioned regions, with the magnitude of impact being dependent on multiple factors including local water demand, abstractions in the river upstream, and the buffering capacity of ancillary water sources to cities. Overall, RFtoIF transition will result in an additional 169.6 million hectares or 22% of the total CONUS land area facing moderate or severe water scarcity. Analysis of just the 53 large urban clusters with 146 million residents shows that the transition will result in 97 million urban population facing water scarcity for at least one month per year on average versus 82 million before the irrigation expansion. While these reported figures are subject to simulation uncertainties despite efforts to exercise due diligence, the study unambiguously underscores the need for strategies aimed at boosting crop productivity to incorporate the effects on water availability throughout the entire extent of the flow networks, instead of solely focusing on the local level. The results further highlight that if irrigation expansion is poorly managed, it may increase urban water scarcity, thus also possibly increasing the likelihood of water conflict between urban and rural areas.

Plain Language Summary

In this study, we investigate the impact of the expansion of irrigation for improving food security on water scarcity. Our results show that the transition of croplands from rainfed to irrigation-fed was found to have an adverse impact on water scarcity in both transitioned and non-transitioned regions. The impacts were influenced by various factors, such as local water demand, abstractions in the river upstream, and the buffering capacity of ancillary water sources to cities. The findings of the study provide valuable insights for policymakers and stakeholders to develop more sustainable strategies that are aimed at boosting crop productivity. Specifically, the study emphasizes the need for devising strategies that consider irrigation expansion's impact on water availability throughout the entire extent of the river network, instead of focusing solely on the local level.

1. Introduction

Increasing population, dietary changes, and growing per capita income are elevating global food demand[1–6]. Considering 2005 as base year, estimates indicate that crop production needs to be roughly doubled to satisfy the food demand by 2050[2]. Several strategies are being practiced or explored to increase the crop productivity and making it more resilient[7–12]. Among these, a prominent option is through the expansion and intensification of irrigated agriculture[13,14]. Irrigation can substantially increase crop yield, and reduce the risks from droughts[15,16]. Given that the share of irrigated cropland in the US was only 16% in 2005, even though it accounted for 44% of the total crop production[17], there is a potential to significantly increase crop productivity through the transition of rainfed agriculture to irrigation-fed in the US. Recognizing this opportunity, several recent studies have explored its potential implications. For example, it was recently reported that transitioning 26% of the current global rainfed land to irrigation-fed can feed an extra 2.8 billion population[13]. Despite its potential, rain-fed to irrigation-fed transition may not always be sustainable, especially if the transition is poorly managed. The irrigation expansion may cause river water depletion, groundwater depletion, and pose a threat to the aquatic ecosystem, thus resulting in freshwater scarcity[18].

In this study, we assess the potential impacts of rain-fed to irrigation-fed (RFtoIF) transition of US croplands on blue water scarcity in the contiguous United States (CONUS). Given that RFtoIF transition is expected to increase the water demand for agriculture in the rural areas, our hypothesis is that it may have an impact on the water supply of domestic and industrial sectors in the urban areas. Here we specifically assess the proliferation of blue water scarcity (see: Methods section), taking into account both the surface and renewable groundwater availability, in large urban clusters (LUCs) (see *Methods: Definition of urban and rural areas*) due to increased agricultural water use from RFtoIF transition in regions which are largely concentrated in rural areas. In contrast to a majority of the past studies concerned with water scarcity evaluations[19–26], and much like a few selected studies[27–29], here we explicitly consider the role of water transfer to urban areas from 316 surface water withdrawal points. However, previous studies have not taken into account the expansion of irrigation in current non-irrigated croplands, instead employing future scenarios that assume an increased demand for irrigation water. This study differs from previous ones in that we assess the impact of the expansion of irrigation on non-irrigated croplands, i.e., the spatial proliferation of blue water scarcity in areas that were not previously irrigated, a topic that has not been addressed in earlier studies. The need for this evaluation is timely especially given the latent potential for irrigation expansion in central and eastern United States, where several regions have already experienced more than 100% increase in irrigation expansion just within 20-years period[30].

2. Methods

2.1. Definition of urban and rural areas

The US Census Bureau delineates geographic areas identifying them as urban or rural. Urban areas represent densely developed aggregations of census blocks, and usually encompass residential, commercial, and other non-residential land uses. Areas not qualifying as urban are coined as rural. Here, the urban-rural area information is obtained from US Census Bureau as TIGER/line Shapefile[31].

In this study, we assess the impact of RFtoIF in 53 large urban clusters (also referred as LUCs henceforth) which are spread over around 11.9 million hectares and populate around 146 million people. The choice of these LUCs is partly motivated by their significant populace, exceeding 750,000, and also due to the availability of comprehensive surface water withdrawal points data for them[29]. Population information for urban regions is obtained from Gridded Population of the World (GPW), SEDAC[32].

2.2. Assessment of blue and green water scarcity

Green water scarcity is assessed using the GWS index which captures the fraction of crop water requirement that is not met by green water, and is obtained as the ratio of monthly irrigation water demand (= crop water requirement – green water use) and crop water requirement[33]. Green water refers to the rainwater and soil moisture consumed by crops. GWS is calculated at monthly resolution using

$$GWS = \frac{CWR - CWSG}{CWR} \tag{4}$$

where, *CWR* is crop water requirement or the amount of water required by a crop to grow optimally, and *CWSG* is the crop water supply from green water. *CWR* and *CWSG* for a given month are calculated by summing daily PET and AET for the month, respectively. GWS is calculated for rainfed crops, therefore, water-limited AET that is solely due to precipitation is used here (see supplementary information for more detail). A region is considered green water scarce if CWSG < 0.9 CWR or in other words, GWS > 0.1 based on Rosa et al.[33].

Blue water scarcity in this study is quantified using the cumulative abstraction to demand (CAD) metric, which is the ratio of water abstraction to water demand[18]. Monthly blue water scarcity is assessed using an index called cumulative abstraction to demand (CAD). CAD is calculated at a monthly time step as the ratio of monthly water abstraction to the demand of all the sectors in the grid cell. Here water abstraction corresponds to abstracted water from both surface and subsurface sources, while the water demand quantifies the total water needed to satisfy the demands of agricultural, domestic, and industrial sectors[34]. When water abstraction in a region is less than the water demand, CAD falls below unity. Generally, CAD < 1 indicates a water shortage, and an alternative source of water is needed to alleviate water scarcity. Smaller is the CAD value, more severe is the scarcity. A low, moderate, high, and severe blue water scarcity corresponds to $0.8 < CAD \leq 0.99$, $0.5 < CAD \leq 0.8$, $0.3 < CAD \leq 0.5$, and $CAD \leq 0.3$, respectively. The water scarcity classification thresholds using CAD are consistent with the other widely used water scarcity indexes- water withdrawal to availability and water availability per capita[35]. Herein, all reported results regarding the regions that face scarcity correspond to $CAD \leq 0.8$, which indicates a moderate to high blue water scarcity, unless explicitly stated otherwise.

2.3. H08 Model Simulations

To assess the impacts of RFtoIF transition on blue water scarcity, a global hydrological model, H08[34], is used to simulate monthly water availability over the CONUS at a spatial resolution of 5 x 5 arcmin. Two scenario simulations are performed. Scenario S1 represents the status quo during 1996-2005, a period around which most of the input data for H08 are available at continental scale (e.g., crop area fraction for 19 crops[36], irrigated area fraction[37], etc.). Scenario S2 simulates the transition of all rain-fed croplands that experience green water scarcity, to irrigation-fed.

The H08 consists of six submodels named land surface, river routing, crop growth, water abstraction, environmental flow, and reservoir operations. H08 was run at daily time intervals and a spatial resolution of 5-arcmin over the period 1996-2005 for the CONUS. All submodels of H08 are coupled to obtain monthly blue water demand for agricultural, industrial, and domestic sectors, and blue water availability in each cell. Blue water demand is satisfied by varied surface and groundwater sources. Surface water is supplied by rivers, canals, reservoirs, and desalination plants while groundwater is supplied from renewable and nonrenewable groundwater resources.

The municipal sector is given priority in water supply, followed by the industrial and agricultural sectors, respectively. Daily meteorological forcing data of precipitation, wind speed, air temperature, air pressure, specific humidity, and longwave and shortwave radiation were obtained from NLDAS[38] at 0.125 degrees, hourly, and downscaled at 5 arc min, daily. Additional non-meteorological input data including irrigated area- area equipped for irrigation (AEI) and area actually irrigated (AAI)[37], cropland area[39], crop area fraction and spatial distribution of 18 selected crops[36], and water withdrawal for domestic and industrial sectors (FAO[40]) were obtained for the year circa 2000. Other relevant data for H08, including parameterizations, were directly obtained based on Hanasaki et al, 2018[41] The EFRs are determined using Shirakawa's (2005) algorithm in which all grids are classified (dry, wet, and stable) based on the monthly minimum and maximum streamflow. [42]

The model divides a grid cell into 4 subcells for the irrigated first-crop area, irrigated second-crop area, rainfed area, and no crop area. Irrigated areas are assumed to support a maximum of two crops, a major crop or the first-crop and a secondary crop as the second-crop. The model estimates daily irrigation water requirements using meteorological forcing, crop and agricultural information (crop intensity, crop type, irrigation efficiency, etc.). Irrigation is applied to the crops to maintain 75% soil saturation. Annual national industrial and municipal water requirements are obtained from the AQUASTAT database[40] and spatially interpolated at 5 arc min according to the population density[32].

H08 incorporates two types of reservoirs, large and medium-sized. Large reservoirs have a catchment area of more than 5000 km^2 and are located on the main river streams and can control the flow. The medium size reservoirs are generally located in the tributaries and act as tank storage, it stores the water until the storage capacity is reached. Any additional water than storage capacity is released to downstream.

The canal water supply system in the H08 enables the grids to transfer water to large distances. H08 considers two types of aqueducts characterized as explicit and implicit. Explicit canals are those that are physically constructed and can be validated by literature, while implicit canals are based on the assumption that the river water is shared with the first neighboring cell. Implicit canals help prevent the artificial gap in water availability for the cells nearby rivers. Due to the unavailability of the continental scale data of explicit canals, the model may underestimate the water abstraction, especially in urban areas. This is alleviated to some extent by the use of city water map data that provides information on the water sources for 53 cities in the US[29]. Large cities abstract water from urban withdrawal points (groundwater, surface water, and desalination plants), some of them are located around a few hundred kilometers away from the cities. Urban water withdrawal point information was implemented in H08 as canal origins.

For both scenarios, S1 and S2, the model[34] allocates water to a grid according to the water demand and availability at the source of water. The available water in any grid is the sum of runoff generated in the grid, renewable groundwater reserve, canal water abstraction, water abstraction from reservoirs, and water released from upstream grids after fulfilling their all-sectoral demands to the grid under consideration. The model also accounts for environmental flow requirements (EFR)[43] as an additional demand, while estimating the blue water scarcity.

2.4. Assessment of intensification and proliferation of blue water scarcity

The total water demand and abstraction in a LUC is calculated by summing the demand of all LUC grids. The ratio between total monthly water abstraction to demand summed over all LUC grids represents CAD for LUCs.

$$CAD_{LUC,m} = \frac{TA_{LUC,m}}{TD_{LUC,m}} \tag{5}$$

where $TA_{LUC,m}$ and $TD_{LUC,m}$ are total monthly water abstraction and demand in LUC grids, respectively, calculated by summing daily industrial (*ind*) and domestic (*dom*) water abstraction (*A*) and demand (*D*) over number of days (*d*) in a month. We did not consider the agricultural water demand in LUC grids due to the presence of small fraction of irrigated croplands in suburban areas. Urban water withdrawal points serve additional source of water abstraction for LUCs. It is assumed that if an urban water withdrawal point is designated to supply water to a city, all the city's grids can abstract water from it based on their demand.

In this study, the intensification of water scarcity is defined as the increase in intensity of blue water scarcity following RFtoIF transition, i.e., areas facing CAD ≤ 0.99 being lower CAD in S2 than in S1. Spatial proliferation of blue water scarcity indicates expansion of areas (or model cells, used interchangeably henceforth) that do not face water scarcity to begin with, i.e., CAD > 0.99 in S1, but do so following RFtoIF transition, i.e., CAD ≤ 0.99 in S2.

3. Results

3.1. RFtoIF transition's impact on sectoral water use and blue water scarcity

In scenario S1, more than 72.8% of the total cropland area or 82.5% of the total rainfed cropland faces green water scarcity for at least one month in a year (Fig. S1). This is consistent with previous studies where 70% of the cropland area was reported to be facing green water scarcity in the CONUS[33] during the same period. Spatially, the GWS magnitude for any given month generally increases with the monthly aridity index (PET/P) (Fig. S2). Areas facing green water scarcity for at least one month a year on average in S1, are considered for RFtoIF transition in S2 (Fig. S3).

Given that freshwater is predominantly shared among agricultural, domestic, and industrial sectors, RFtoIF transition alters water availability, and consequently, water withdrawal by all three sectors. Specifically, irrigation expansion causes an increase in annual average agricultural water demand over the simulation period, with total water withdrawal increasing from 318 million m^3 per day to 1119 million m^3 per day after the RFtoIF transition (Fig. S4). The largest increase takes place in the summer (Table 1). Notably, the increase in agricultural water use results in less water available for industrial and domestic water use, resulting in a reduction from 600 million m^3 per day to 587 million m^3 per day.

Next, we assess the average monthly blue water scarcity for both scenarios. The difference in CAD, after and before the RFtoIF transition shows the impact of transition on blue water scarcity (Fig.1). The land area facing at least a moderate annual average blue water scarcity (CAD ≤ 0.8) increases from 71.5 million ha (~ 9.33% of the total land area in CONUS) to 241.08 million ha (~ 31.45% of the total land area), i.e., an increase of 169.6 million ha, after RFtoIF transition (see definitions of blue water scarcity severities in *Methods: Assessment of blue and green water scarcity*). The spatial distribution of blue water scarcity varies monthly, and peaks in spring and summer largely because of the increased water demand during this period. The impact is maximum during the month of August, when the land area facing moderate blue water scarcity increases from 68.6 million ha (~ 9% of the total land area in CONUS) to 228.7 million ha (~ 30% of the total land area) after RFtoIF transition. In S1, around 27% and 66% of the CONUS face blue water scarcity that is at least moderate (CAD $\leq$ 0.8) and low (CAD $\leq$ 0.99) in intensity for at least one month, respectively. The corresponding values increase to 49% and 76% after the RFtoIF transition. The scarcity intensification is largest in High Plains, with Texas, Kansas, and Nebraska experiencing intensification in the majority of months. Significant expansion is also experienced in the eastern US, which has low or no water scarcity in scenario S1. California, Oklahoma, Iowa, Indiana, South Dakota, North Dakota, Minnesota, Illinois, and Missouri observe the spatial proliferation of blue water scarcity, mainly in the summer (Fig. 1). The somewhat conspicuous reduction of CAD in North Dakota in winter is due to a reduction in water availability for industrial and domestic sectors, which in turn is a result of upstream usage of water for irrigation of winter crops in Montana following RFtoIF transition. Notably, the water reduction in North Dakota is small but the change in CAD is high due to the small water demand. Some areas of Mississippi and Arkansas that contribute to the lower Mississippi river basin also show an increase in blue water scarcity in the summer after the RFtoIF transition.

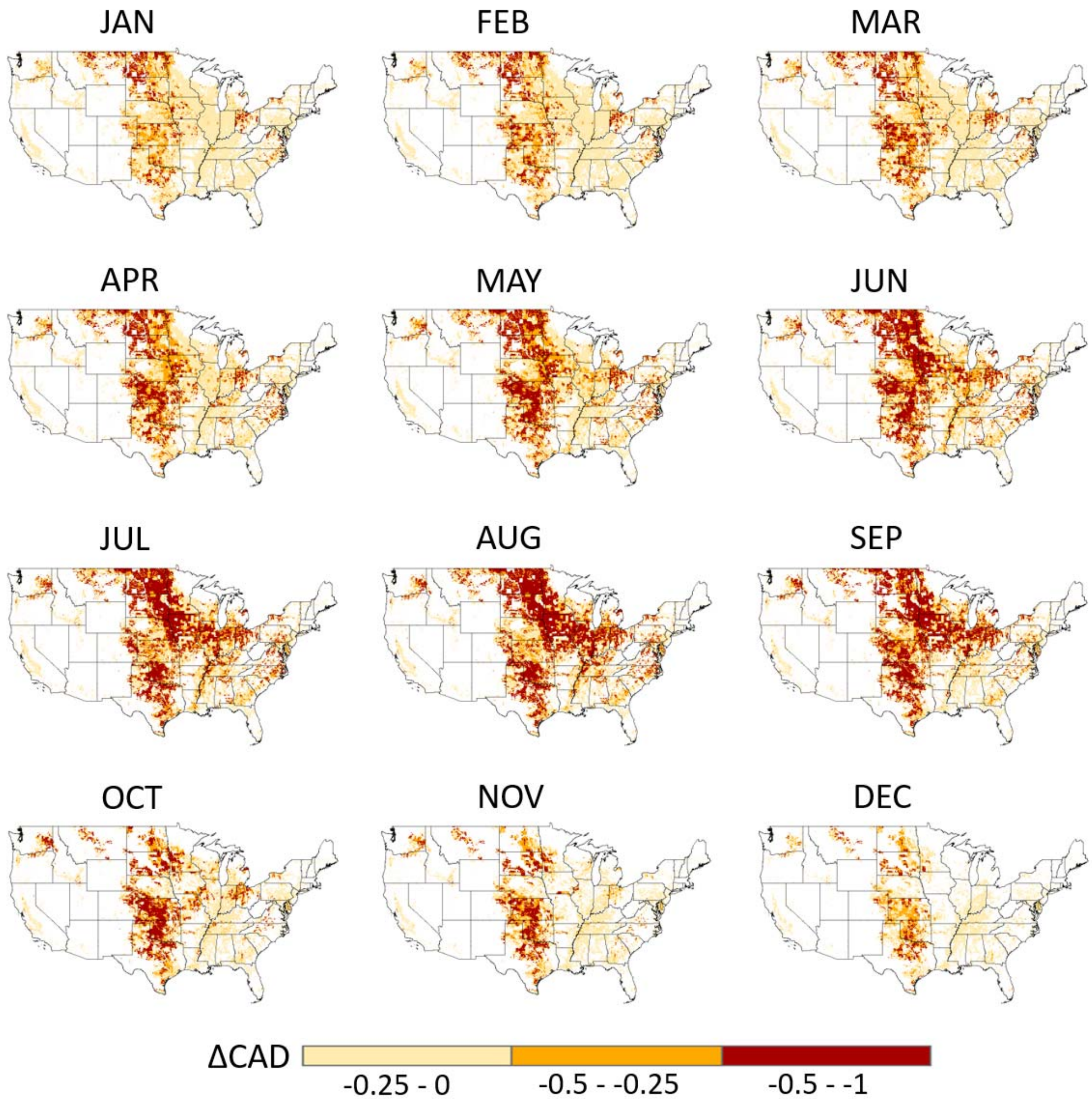

Figure 1. Spatial distribution of the difference in CAD (ΔCAD) after and before the RFtoIF transition. Negative values indicate a decrease in CAD (or an increase in blue water scarcity) with RFtoIF transition.

RFtoIF transition is expected to generally increase blue water scarcity in areas undergoing transition because of the extra water usage in irrigation. The aggravated blue water scarcity in the transitioned area indicate that existing renewable water resources (i.e., the river discharge or reservoirs) and water transportation infrastructure (i.e., implicit and explicit aqueducts, and urban water withdrawal points, (see *Methods: H08 Model*)) are inadequate for fulfilling the increased water demand due to RFtoIF transition. Notably, the RFtoIF transition also causes a rise in monthly blue water scarcity in the areas untouched by the transition. This is because an increase in agricultural water withdrawal from surface water sources due to irrigation expansion in upstream areas leads to a reduction in water flow in river channels, and hence less water availability in receiving lakes and reservoirs. Notably, the average annual surface water use for irrigation increases from 162 million m^3 per day to 517.8 million m^3 per day after RFtoIF transition.

The impact can be gauged both in terms of intensification and spatial proliferation of blue water scarcity. Around 5.3 million hectares (27.2 million hectares) of land that did not undergo RFtoIF transition in S2 face spatial proliferation (intensification) in blue water scarcity (Fig. S5).

3.2. RFtoIF transition and the urban water security

RFtoIF transition, which is primarily concentrated in rural areas (see definition in rural areas in *Methods: Definition of urban and rural areas*) with 97% of the RFtoIF transitioned land lying within it, may have significant impacts on the urban water security. Analyses of blue water scarcity over LUCs (see *Methods: Water Supply Data of LUCs*) for which detailed data of water supply infrastructure is publicly available, show evidence of both spatial proliferation and intensification of blue water scarcity in them. CAD estimates over LUCs are evaluated to assess the differential impacts of RFtoIF transition on them. The impact of RFtoIF transition is significant in LUCs, with spatial proliferation (intensification) of blue water scarcity increasing by 0.97 million hectares (8.2 million hectares), i.e. around 4.4% (37.5%) of the total area of LUCs considered in this study. Before RFtoIF transition, i.e., in scenario S1, 86.2% of LUC and 90.2% of rest of the area (henceforth referred to as ROA) model cells have CAD values greater than 0.8, which belongs to a low or no water scarcity category (Fig. 2). After the RFtoIF transition, the percent of cells that face no or low water scarcity reduces to 84.3% and 67.8% for LUCs and ROA, respectively. In contrast, 13% of the total ROA cells are estimated to face a moderate blue water scarcity after the transition, while it was 5.3% in S1. The LUCs also see a hike in the number of cells facing moderate blue water scarcity after transition with fractional area rising to 9.2% from 7.8%.

Results show that 24 (18) out of 53 highly populated LUCs face a blue water scarcity with at least a moderate intensity for a minimum of one month (six months), respectively (Fig. 3) before RFtoIF transition. These 24 urban areas have a population of around 82 million and roughly constitute 25% of the total US population. The number rises to 29 cities facing blue water scarcity for at least one month with a population of around 97 million urban population or 29.5% of the US population after the RFtoIF transition. In addition, urban agglomerations of Columbus in OH, Dallas--Fort Worth--Arlington in TX, Houston in TX, Memphis in TN—MS—AR, Minneapolis--St. Paul in MN—WI, and Virginia Beach in VA face moderate water scarcity ($0.5 < CAD \leq 0.8$) for at least

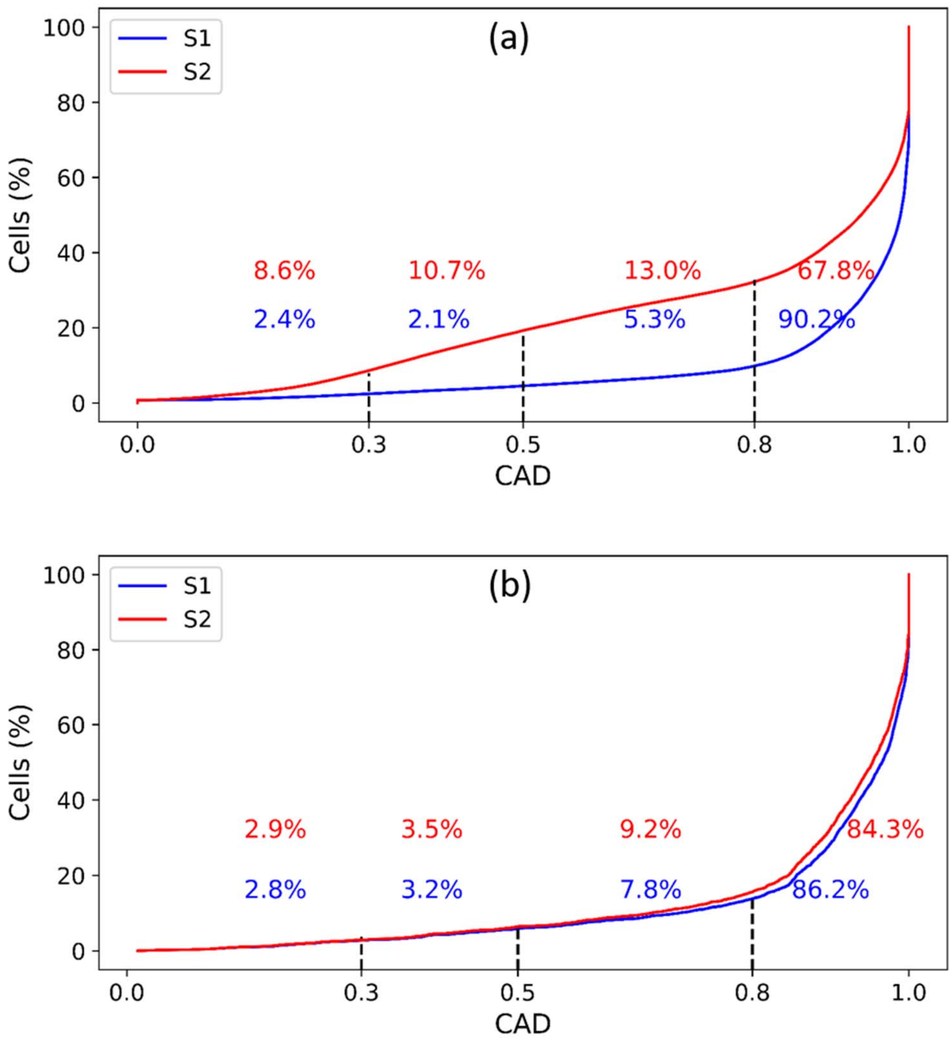

Figure 2. Cumulative distribution function of CAD values for ROA (a), and LUC cells (b) for scenarios S1 (blue) and S2 (red). The numbers indicate the percent of cells belonging to different blue water scarcity classes i.e. low ($0.8 < \text{CAD} \leq 0.99$), moderate ($0.5 < \text{CAD} \leq 0.8$), high ($0.3 < \text{CAD} \leq 0.5$), or severe ($\text{CAD} \leq 0.3$). Fraction of the cells with low or no water scarcity reduces after the RFtoIF transition in both LUCs and ROA. The reduction in fraction of ROC cells is relatively larger.

one extra month after RFtoIF transition. Overall, RFtoIF transition increases scarcity in 6 out of 53 urban areas, affecting additional 16 million people.

3.3. Variables that influence the spatial distribution and intensity of blue water scarcity, and changes in it due to RFtoIF transition

The spatial distribution of CAD is found to be largely controlled by the relative availability of water from upstream. Locations (or model cells) receiving high incoming lateral flow or runoff

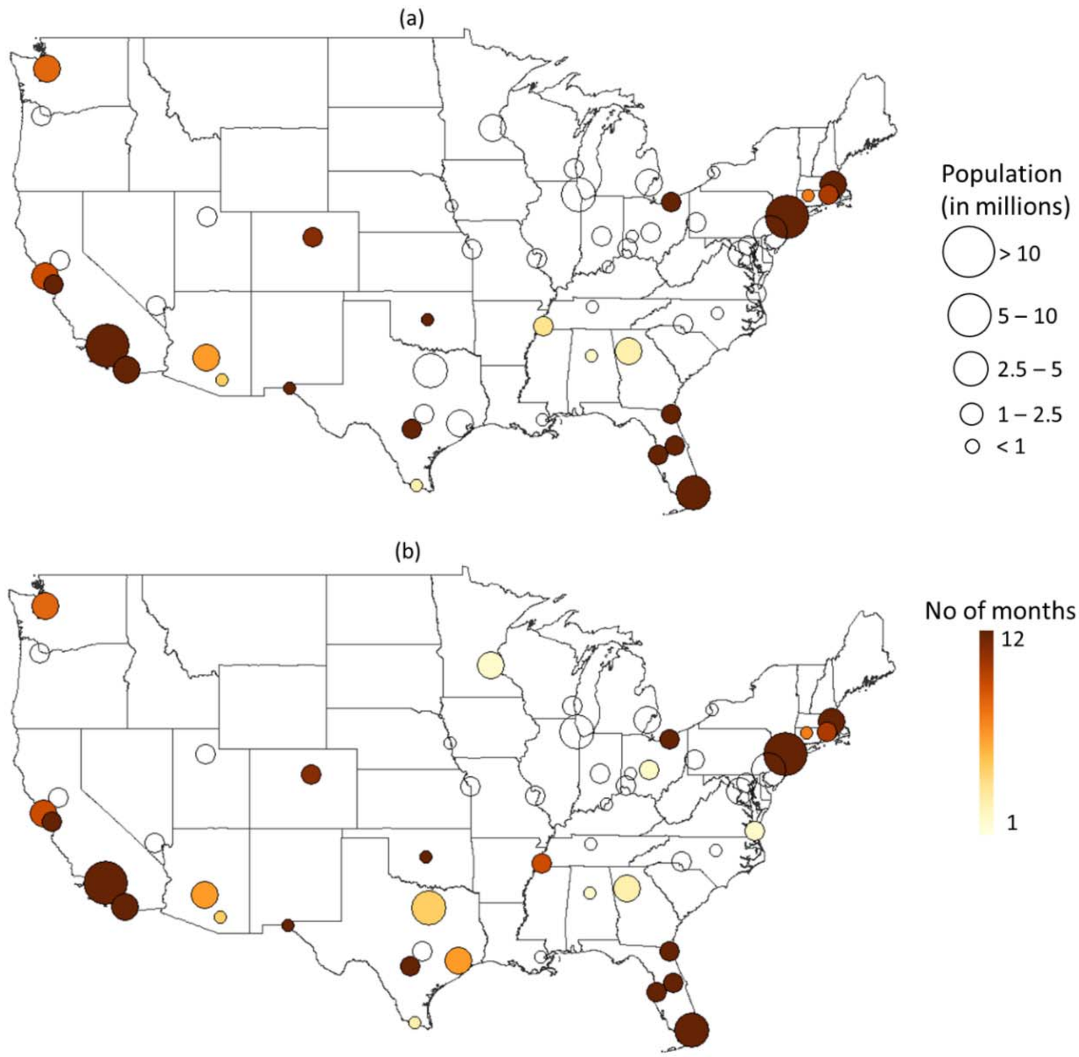

Figure 3. Blue water scarcity for 53 LUCs for scenarios S1 (a) and S2 (b). The size of the circle represents the population, and the color represents the number of months a LUC faces water scarcity

generally have higher CAD values or low blue water scarcity (Fig. 4a). For example, among cells with CAD ≤ 0.5, around 55% of them have a lateral flow of less than 0.0001 MCM per day. Further, 59% of the severely water scarce cells, i.e., CAD ≤ 0.3, have lateral flow less than 0.0001 MCM per day. For ROA cells, CAD distribution is affected by crop area as well, as water demand increases with high crop area. The difference between potential evapotranspiration (PET) and actual evapotranspiration (AET), which captures the irrigation water demand for crops, is another influencing factor. Together, it is observed that cells with less PET-AET and less crop area generally have higher CAD values (Fig. 4b for scenario S2). In contrast, for LUC cells that usually do not have any significant fraction of croplands, the water demand and consequently the CAD is influenced by the human population. Cells with less population and less lateral flow tend to show higher CAD values or less blue water scarcity (Fig. 4d).

The change in blue water scarcity, as quantified by ΔCAD, is either zero or negative. Of the LUC cells that experience a change in CAD, most observe ΔCAD between 0 to -0.2 (Table 2 and Fig S6). The same is true for non-transitioned ROA cells. Among the ROA cells that undergo transition, a large fraction of them (> 70%) have ΔCAD < -0.2. Around 5.7% of the transitioned grids have ΔCAD ranging from -1 to -0.8. Overall, when all cells are considered, more than 24% of the cells experience ΔCAD < -0.2.

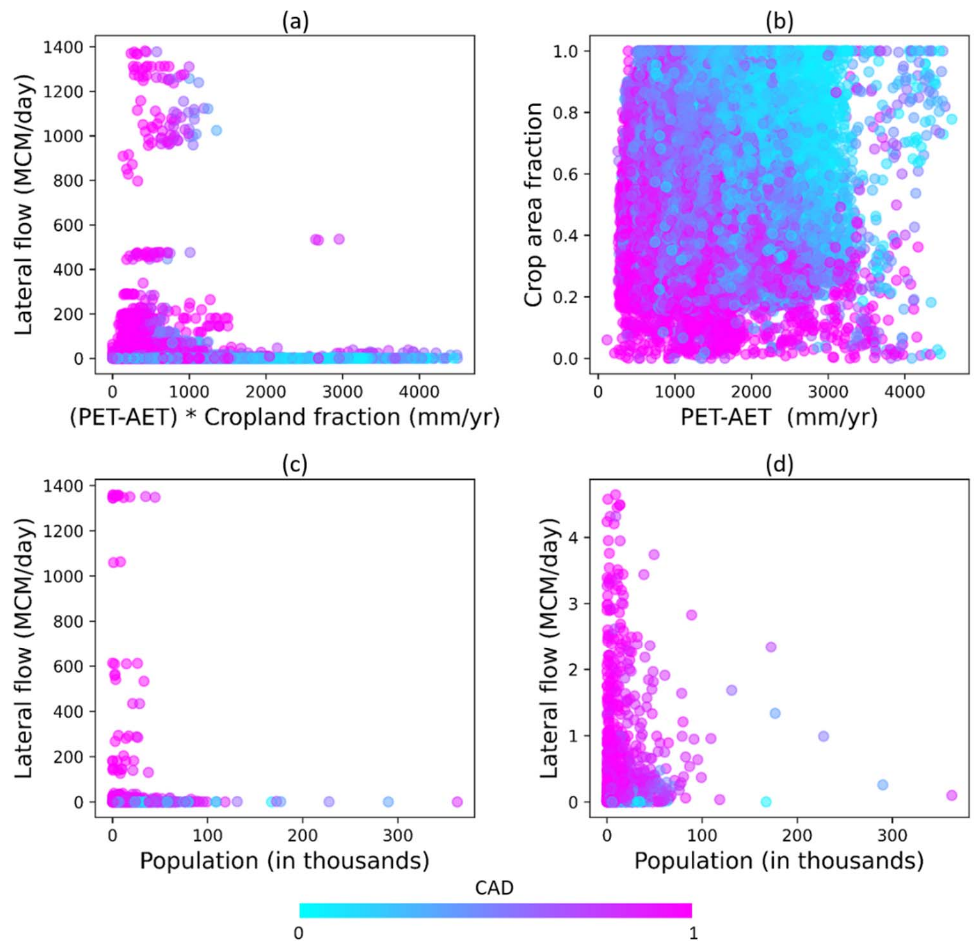

Figure 4. (a) Lateral flow for ROA cells vs. ((PET-AET)*crop area). PET is the potential evapotranspiration and AET is the actual evapotranspiration. ((PET-AET)*crop area) represents the crop water demand in a cell. (b) ROA cells with lateral flow less than 1 MCM/day show smaller CAD, with CAD generally decreasing with higher (PET-AET) and crop area fraction. (c) Lateral flow for LUC cells vs. population. (d) LUC cells with lateral flow less than 5 MCM/day show an increase in blue water scarcity (or decrease in CAD) with increasing population. The data in all the subplots is for the month of June only.

To understand the influences on the spatial distribution of ΔCAD, ΔCAD for LUC and ROA cells are expressed as:

$$\Delta CAD = \frac{A2}{D2} - \frac{A1}{D1} = \frac{A2 - A1}{D2} - \frac{A1}{D2.D1}(D2 - D1)$$
$$= \frac{(A2 - A1) - \frac{A1}{D1}(D2 - D1)}{D2} \quad (1)$$

$$\Rightarrow \Delta CAD = \frac{\Delta abs - \frac{A1}{D1} * \Delta dem}{D1 + \Delta dem} \quad (2)$$

where, *A1* and *D1* (*A2* and *D2*) are the water abstraction and demand in scenario S1 (S2), respectively. Δ*abs* (= *A2-A1*) and Δ*dem* (= *D2-D1*) represent the change in water abstraction and demand due to transition, respectively. Δ*dem* is either zero or positive while Δ*abs* is either negative or positive depending on the availability of excess water available for abstraction following RFtoIF transition.

For LUCs, since the water demand remains the same in both scenarios because of the absence of RFtoIF transition in them, Δ*dem* is zero and the equation 2 reduces to:

$$\Delta CAD = \frac{\Delta abs}{D1} \quad (3)$$

As indicated in Equation 3, ΔCAD increases as the magnitude of Δ*abs* increases for LUC cells (Fig. 5a). For a given Δ*abs*, high-demand LUCs that are primarily the areas with high population density or industrialization experience smaller change in CAD or blue water scarcity. Conversely, ΔCAD is generally higher for urban areas which a higher reduction in water abstraction (Fig. S7. LUCs with higher Δ*abs* either face water scarcity for additional months or experience a reduction in CAD value after the transition. For example, Houston, TX receives water from Lake Livingston on the Trinity River, and Lake Houston and Lake Conroe on the San Jacinto River, for its daily domestic and industrial needs and does not face water scarcity in S1.

After irrigation expansion in scenario S2, predicted water availability in current surface water sources reduces and the existing water transport infrastructure is unable to meet the city water demands. Thus, the number of water-scarce months rises to 6 in S2. The largest reduction in water abstraction is observed in September, when it reduces by around 10%. The mean annual water abstraction reduces by around 4%. Consequently, CAD reduces for all the months. blue water scarcity changes from no or low to moderate for May-Oct. A similar picture unfolds in Dallas, where water scarcity months rise from 0 to 4 due to reduced water availability in the city's water

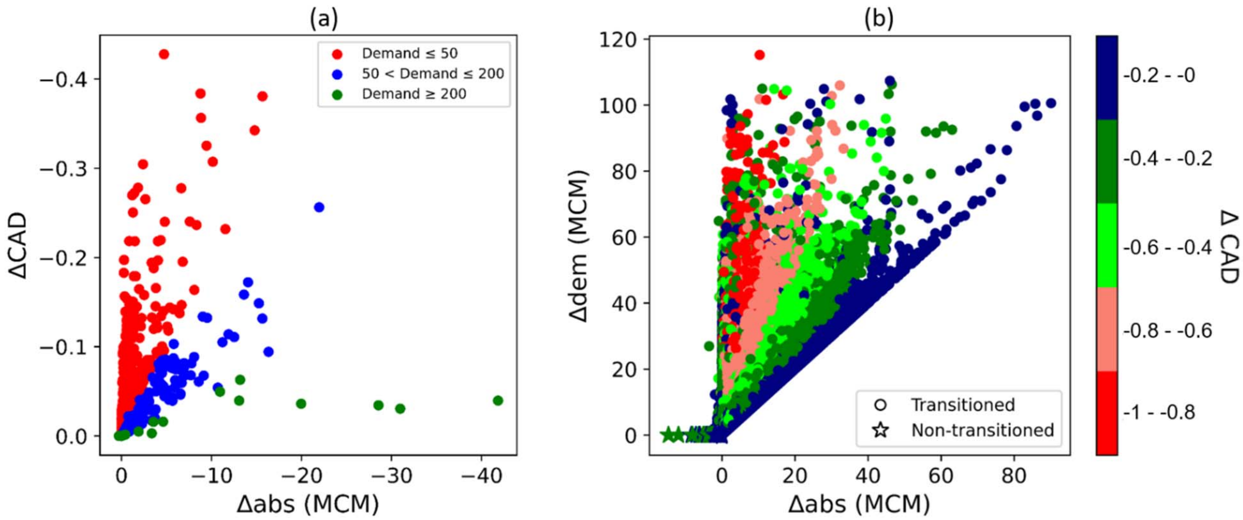

Figure 5. (a) Scatter plot between annual average ΔCAD and Δabs for LUC cells. Cells with higher demand (shown in million cubic meter per year (MCM/year)) have smaller ΔCAD for the same Δabs, (b) annual average Δabs and Δdem scatter plot for ROA cells. Some of the non-transitioned cells show change in CAD even after no change in demand in scenario S2. For transitioned grids, change in CAD is higher for the cells with less increase in abstraction i.e. low Δabs, while cells with high Δabs have less change in CAD.

resources. Along similar lines, Columbus, OH; Memphis, TN—MS—AR; Minneapolis--St. Paul, MN—WI; and Virginia Beach, VA have large absolute Δabs and face at least one additional month of water scarcity. Notably, urban agglomerations with sufficient excess water supply and/or minimal RFtoIF transition upstream manage to be unaffected by RFtoIF transition. For example, two major urban agglomerations in Arizona, viz. Phoenix-Mesa and Tucson experience blue water scarcity for 6 and 4 months, respectively, in both scenarios S1 and S2, as relatively small increase in water withdrawal from RFtoIF transition can be supplemented by water supply from Central Arizona Project (CAP) reservoirs (Tucson and Phoenix-Mesa) and Salt Lake Project (Phoenix-Mesa). In a few circumstances, number of months experiencing changes in scarcity may be zero because they may already be scarced in all months in scenario S1. For ecample, New York—Newark, Oklahoma City, and San Antonio, already experience a full year of water scarcity, indicating that no further months are added in those cities. It is to be noted that for several LUCs, such as Milwaukee, Kansas City, Chicago, and St. Louis, while RFtoIF transition in the upstream contribution area decreased river flow causing negative change in abstraction from it (Fig. 6, local water sources in the neighborhood that supply water through canals are able to cushion this reduction (as indicated by positive change in abstraction from canals). In contrast, LUCs that experience increase in number of months of scarcity generally experience negative change abstraction from both rivers and the canals. This highlights that the impact of RFtoIF transition on scarcity can be mediated by anciallary water sources that are not directly or significantly impacted by RFtoIF transition.

For ROA cells, in addition to Δ*abs* and D1, the spatial distribution of ΔCAD is controlled by additional variables including Δ*dem* and A1 (see Equation 2). Notably, among the ROAs, most transitioned locations have positive Δabs, while the non-transitioned cells either have zero or negative Δabs (Fig. 5b). This suggests that transitioned cells withdraw more water to match the demand after RFtoIF transition, while cells that do not participate in transition withdraw less or the same amount of water depending on the extent of reduction in water availability at the location. ΔCAD for non-transitioned ROA cells behaves like that of LUC cells, with its absolute value increasing with an increase in Δabs. In contrast, at the transitioned ROA locations, the absolute value of ΔCAD decreases with an increase in Δabs magnitude for a given Δdem. In other words, if the increase in abstraction does not match the increase in water demand, transitioned locations experience higher ΔCAD.

4. Discussion and Synthesis

It is well known that transitioning from rainfed to irrigation-fed agriculture boosts crop yields and improves food security. Our continental hydrologic simulation, however, shows that RFtoIF transition over croplands that experience green water scarcity for an average of at least one month a year intensifies freshwater scarcity in both transitioned and non-transitioned areas. Notably, urban areas that generally support significant populations also experience increased water scarcity due to an increase in agricultural water usage by upstream rural users. Our simulation results show that from among just the 53 considered LUCs, around 16 million additional urban residents will get affected by such a transition. This may increase the risk of water conflict between urban and the surrounding upstream rural water users, as it is being realized in many water stressed situations throughout the world[44–48].

The analysis was conducted assuming all rainfed areas facing green water scarcity for at least one month are converted to irrigation fed, which while being an unlikely scenario in terms of its implementation, helps highlight the degree of impact that may be incurred. The study does not account for water consumption by poultry and livestock in agricultural sectors. The impact of RFtoIF transition on the increase in the number of livestock and consequently water use by them[49] is also not considered here. A model facilitating livestock and other farm water consumption may be used to assess the overall impact. However, the water use by livestock is minimal as compared to other sectors (less than 1% of total freshwater withdrawals in 2000)[50].

The water scarcity evaluations performed here are based on the historical datasets, i.e. crop area distribution and irrigated area maps circa 2000 and 2005, respectively. Given that new and better data is continuously being generated, the reported population facing blue water scarcity in the status quo and transition scenario are expected to change with their usage. It is also to be noted that by the year the full RFtoIF transition (as simulated in S2) may get realized, if it ever does, the climate is likely to be different. However, given the uncertainty in timeline of this transition, the current study does not consider the concomitant impacts of changes in climate on evapotranspiration, precipitation, water availability, and water demand[51,52]. During the transition, other socioeconomic changes such as urban and rural demographics, water infrastructure technology, economic changes, changes in water withdrawal efficiency for all three sectors, cropping patterns, agricultural management practices, land cover change, etc. are subject to change and may affect the water scarcity in an area as well. These factors are not explicitly considered in

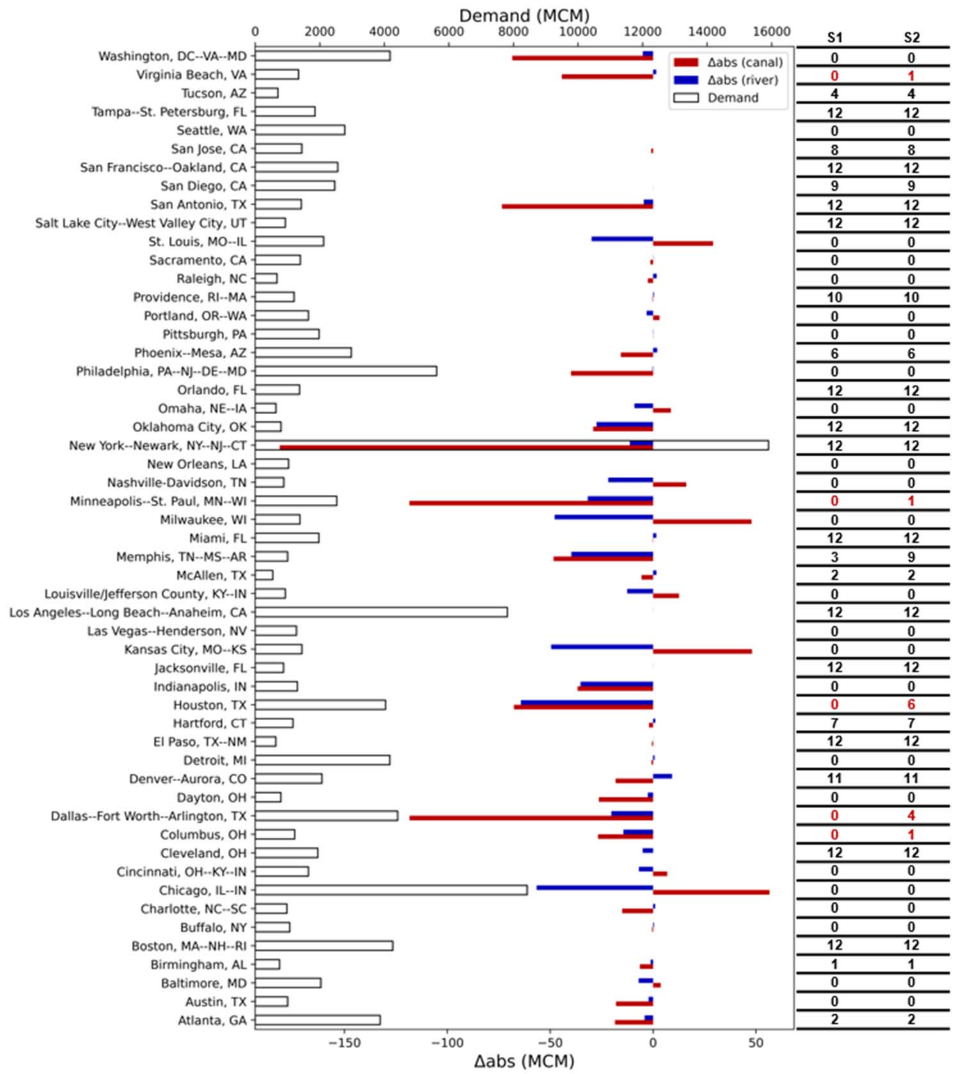

Fig. 6. 53 LUCs considered in this study and their average annual water demand and Δabs. The Δabs is specified separately based on the source of water abstraction i.e. river and canal. Water abstraction from WTPs is included in canal water abstraction. Column on the right indicates number of months of water scarcity in scenarios S1 and S2 for each considered LUC.

the scenario simulations performed here. We further acknowledge that the RFtoIF transition may disturb local hydrological cycle and affect the precipitation, evapotranspiration, surface temperature, and other land atmospheric interactions[53–55]. These factors can affect the water scarcity estimates well.

It is to be noted that just as is the case with most model implementations, the H08 model results, which have been used to obtain the scenario simulations in this study, suffer from model structure and data uncertainty. For example, as the model does not consider lateral groundwater flow between cells, it may have impacted the estimates of the spatial distribution of CAD and ΔCAD as groundwater withdrawals may directly impact the surface water resources[56,57]. Uncertainties also exist in terms of accounting for all the possible surface water supplies. An effort has been made in this study to reduce this uncertainty by including urban water withdrawal points[29]. A more accurate dataset on distant water supply may improve the results. Notably, only surface urban withdrawal points were considered, due to their ability to be incorporated as canal origin points in the current version of H08. This may result in an overestimation of blue water scarcity in cities that rely primarily on groundwater or desalinization for their municipal and industrial water demand. Another source of uncertainty may arise due to the current representation of urban water withdrawal points in H08. Specifically, while all LUC grids are able to abstract water from urban withdrawal points, the grids that come first in the pre-defined sequence are prioritized for withdrawal. This could potentially impact water scarcity at the grid scale, although the overall effect on the LUC level is likely to be minimal as the abstraction from all grids is aggregated to calculate the total water abstracted by the LUCs. Furthermore, the study assumes that the domestic sector is the first to extract water, followed by the industrial and then the agricultural sectors. Assuming agriculture has the lowest priority in water abstraction is a pragmatic choice given the lack of information on which regions prioritize which sectors. However, the results of water scarcity can be sensitive to this assumption. According to Flörke et al.[28], climate change affects the surface water deficit in urban areas in significantly different ways depending on the water extraction priority assigned to the urban population.

In this study, areas facing water scarcity are derived using the CAD index. The index is similar to other commonly employed water scarcity indices such as the criticality ratio[58], Falkenmark index[20], and water footprint based index. Previous studies[35,59] have shown that estimates of population experiencing scarcity are only mildly sensitive to the choice of water scarcity metrics (Table S1a), and there is a close correspondence between these indices. This is unsurprising as majority of these metrics use two similar primary variables, namely the abstracted water amount or the water available for abstraction, and demand or water footprint (Table S1b). Differences between metrics may arise from the inclusion of additional variables, such as accounting of water-use losses in water abstraction term or the numerator of CAD. The magnitude of these additional variables can lead to variations in the estimates of water scarcity across metrics. It's worth noting that each metric often applies subjective thresholds to classify the severity of scarcity, which can also contribute to disparities in results between metrics.

Apart from these, uncertainties may also occur due to the use of spatially uniform irrigation and, domestic and industrial water use efficiencies, which are set to 0.6, 0.15, and 0.1, respectively, over all the cells. Furthermore, the results are based on a temporally static distribution of irrigation area, cropland-pasture fraction, and areas of different crops over the simulation period. The industrial and domestic water withdrawal used in this study is obtained from AQUASTAT and downscaled to the modeling scale of 5x5 arcmin based on the population distribution. Notably, the temporal variation of domestic and industrial water withdrawal is also not taken into consideration. This issue can be attenuated if the model is supplied with more accurate data on water withdrawal by domestic and industrial sectors. Notably, the first priority for water abstraction is given to the domestic sector followed by the industrial and agricultural. As an earlier study[28] has reported, water scarcity in urban areas is sensitive to the water supply preferences, the results may change if other sectors are prioritized. CAD and ΔCAD estimates are likely to be also affected by uncertainties in EFR, which here is defined based on the monthly average river discharge[42]. Studies[60] have previously reported that the EFR estimation method may determine water scarcity assessment, although Mekonnen and Hoekstra (2016)[19] also noted that the population living under moderate blue water scarcity does not change significantly for the uncertainty range of EFR. Another source of uncertainty is from the current AET and PET parameterizations, which do not account for crop-specific stomatal conductances. Given that these conductances may vary with crops and cultivars[61], uncertainties in PET and ET estimates can be reduced by performing calibration and validation against remotely-sensed evapotranspiration estimates[62].

Despite the aforementioned methodological limitations, the analysis clearly shows that the controls on changes in blue water scarcity (or ΔCAD) are different between non-transitioned and transitioned locations. The trend of changes in ΔCAD vis-à-vis changes in abstraction is also contrasting between non-transitioned and transitioned locations. In addition, the affect of RFtoIF transition on urban areas, especially in regards to additional months being affected by scarcity is dependent both on antecedent scarcity state before transition and presence of ancillary water supply sources to cities either from reservoirs or locations that are not directly impacted bt RFtoIF transition. Overall, the study indicates that the irrigation expansion, if not properly managed, is unsustainable. Furthermore, irrigation expansion can enhance water scarcity in large urban areas and could be a conflict agent between urban and rural water users. Given the existing significant divide in the urban-rural electorate in US[63], these conflicts are likely to get aggravated and spur social and administrative challenges regarding water allocation and access. Alterations in water resources due to rapid urbanization, and socio-economic and climate change, are likely to further pose challenges for water managers[64–66]. Since the impacts of RFtoIF transition propagate downstream, constraining urban-rural conflicts[44–48] may require update and/or formulation of innovative basin-scale water apportioning doctrines and compacts.

Acknowledgements

MK acknowledges support from the National Science Foundation (NSF, grant nos. EAR-1856054 and OIA-2019561).

Author Contributions

MK conceived the study, acquired funding, and provided project administration and supervision. LR compiled the data, performed model simulations, developed relevant codes for analyses and visualizations, and generated model outputs. LR and MK designed the methodology, performed data analyses, and drafted the manuscript. NH and PR contributed to model implementation. All authors edited the manuscript and helped improve it.

Competing Interests

The authors declare no competing interests.

Open Research

Data analyses were performed using Python (version 3.8), major libraries used are: pandas, numpy, scipy, os, glob, arcpy, geopandas, and matplotlib. The datasets generated and/or analysed during the current study are available in the Zenodo repository (see link: https://zenodo.org/record/7641692).

References

1. Godfray, H. C. J. *et al.* Food Security: The Challenge of Feeding 9 Billion People. *Science* **327**, 812–818 (2010).

2. Tilman, D., Balzer, C., Hill, J. & Befort, B. L. Global food demand and the sustainable intensification of agriculture. *Proc. Natl. Acad. Sci.* **108**, 20260–20264 (2011).

3. Beltran-Peña, A., Rosa, L. & D'Odorico, P. Global food self-sufficiency in the 21st century under sustainable intensification of agriculture. *Environ. Res. Lett.* **15**, 095004 (2020).

4. Foley, J. A. *et al.* Solutions for a cultivated planet. *Nature* **478**, 337–342 (2011).

5. Cirera, X. & Masset, E. Income distribution trends and future food demand. *Philos. Trans. R. Soc. B Biol. Sci.* **365**, 2821–2834 (2010).

6. Garnett, T. *et al.* Sustainable Intensification in Agriculture: Premises and Policies. *Science* **341**, 33–34 (2013).

7. Richards, R. A., Rebetzke, G. J., Condon, A. G. & van Herwaarden, A. F. Breeding Opportunities for Increasing the Efficiency of Water Use and Crop Yield in Temperate Cereals. *Crop Sci.* **42**, 111–121 (2002).

8. Raines, C. A. Increasing Photosynthetic Carbon Assimilation in C3 Plants to Improve Crop Yield: Current and Future Strategies. *Plant Physiol.* **155**, 36–42 (2011).

9. Smith, R. G., Gross, K. L. & Robertson, G. P. Effects of Crop Diversity on Agroecosystem Function: Crop Yield Response. *Ecosystems* **11**, 355–366 (2008).

10. Wang, Y. *et al.* Effects of rainfall harvesting and mulching technologies on water use efficiency and crop yield in the semi-arid Loess Plateau, China. *Agric. Water Manag.* **96**, 374–382 (2009).

11. Blum, A. Effective use of water (EUW) and not water-use efficiency (WUE) is the target of crop yield improvement under drought stress. *Field Crops Res.* **112**, 119–123 (2009).

12. Su, Z. *et al.* Effects of conservation tillage practices on winter wheat water-use efficiency and crop yield on the Loess Plateau, China. *Agric. Water Manag.* **87**, 307–314 (2007).

13. Rosa, L. *et al.* Closing the yield gap while ensuring water sustainability. *Environ. Res. Lett.* **13**, 104002 (2018).

14. Rosa, L. *et al.* Potential for sustainable irrigation expansion in a 3 °C warmer climate. *Proc. Natl. Acad. Sci.* **117**, 29526–29534 (2020).

15. Troy, T. J., Kipgen, C. & Pal, I. The impact of climate extremes and irrigation on US crop yields. *Environ. Res. Lett.* **10**, 054013 (2015).

16. Zaveri, E. & B. Lobell, D. The role of irrigation in changing wheat yields and heat sensitivity in India. *Nat. Commun.* **10**, 4144 (2019).

17. Alexandratos, N. World Agriculture towards 2030/2050: the 2012 revision. 154.

18. Hanasaki, N. *et al.* An integrated model for the assessment of global water resources – Part 2: Applications and assessments. *Hydrol. Earth Syst. Sci.* **12**, 1027–1037 (2008).

19. Mekonnen, M. M. & Hoekstra, A. Y. Four billion people facing severe water scarcity. *Sci. Adv.* **2**, e1500323 (2016).

20. Falkenmark, M. The Massive Water Scarcity Now Threatening Africa: Why Isn't It Being Addressed? *Ambio* **18**, 112–118 (1989).

21. Falkenmark, M., Lundqvist, J. & Widstrand, C. Macro-scale water scarcity requires micro-scale approaches. *Nat. Resour. Forum* **13**, 258–267 (1989).

22. Oki, T. & Kanae, S. Global Hydrological Cycles and World Water Resources. *Science* **313**, 1068–1072 (2006).

23. Vörösmarty, C. J., Green, P., Salisbury, J. & Lammers, R. B. Global Water Resources: Vulnerability from Climate Change and Population Growth. *Science* **289**, 284–288 (2000).

24. Alcamo, J. & Henrichs, T. Critical regions: A model-based estimation of world water resources sensitive to global changes. *Aquat. Sci.* **64**, 352–362 (2002).

25. Wada, Y. *et al.* Global monthly water stress: 2. Water demand and severity of water stress. *Water Resour. Res.* **47**, (2011).

26. Hoekstra, A. Y., Mekonnen, M. M., Chapagain, A. K., Mathews, R. E. & Richter, B. D. Global Monthly Water Scarcity: Blue Water Footprints versus Blue Water Availability. *PLOS ONE* **7**, e32688 (2012).

27. He, C. *et al.* Future global urban water scarcity and potential solutions. *Nat. Commun.* **12**, 4667 (2021).

28. Flörke, M., Schneider, C. & McDonald, R. I. Water competition between cities and agriculture driven by climate change and urban growth. *Nat. Sustain.* **1**, 51–58 (2018).

29. McDonald, R. I. *et al.* Water on an urban planet: Urbanization and the reach of urban water infrastructure. *Glob. Environ. Change* **27**, 96–105 (2014).

30. Walton, B. U.S. Irrigation Continues Steady Eastward Expansion. *Circle of Blue* https://www.circleofblue.org/2019/world/u-s-irrigation-continues-steady-eastward-expansion/ (2019).

31. Bureau, U. C. TIGER/Line Shapefiles. *The United States Census Bureau* https://www.census.gov/geographies/mapping-files/time-series/geo/tiger-line-file.html.

32. Center For International Earth Science Information Network-CIESIN-Columbia University. Gridded Population of the World, Version 4 (GPWv4): Population Count, Revision 11. (2018) doi:10.7927/H4JW8BX5.

33. Rosa, L., Chiarelli, D. D., Rulli, M. C., Dell'Angelo, J. & D'Odorico, P. Global agricultural economic water scarcity. *Sci. Adv.* **6**, eaaz6031 (2020).

34. Hanasaki, N. *et al.* An integrated model for the assessment of global water resources – Part 1: Model description and input meteorological forcing. *Hydrol. Earth Syst. Sci.* **12**, 1007–1025 (2008).

35. Hanasaki, N., Yoshikawa, S., Pokhrel, Y. & Kanae, S. A Quantitative Investigation of the Thresholds for Two Conventional Water Scarcity Indicators Using a State-of-the-Art Global Hydrological Model With Human Activities. *Water Resour. Res.* **54**, 8279–8294 (2018).

36. Monfreda, C., Ramankutty, N. & Foley, J. A. Farming the planet: 2. Geographic distribution of crop areas, yields, physiological types, and net primary production in the year 2000. *Glob. Biogeochem. Cycles* **22**, (2008).

37. Siebert, S. *et al.* A global data set of the extent of irrigated land from 1900 to 2005. *Hydrol. Earth Syst. Sci.* **19**, 1521–1545 (2015).

38. Xia, Y. *et al.* Continental-scale water and energy flux analysis and validation for the North American Land Data Assimilation System project phase 2 (NLDAS-2): 1. Intercomparison and application of model products. *J. Geophys. Res. Atmospheres* **117**, (2012).

39. Ramankutty, N., Evan, A. T., Monfreda, C. & Foley, J. A. Farming the planet: 1. Geographic distribution of global agricultural lands in the year 2000. *Glob. Biogeochem. Cycles* **22**, (2008).

40. AQUASTAT database. http://www.fao.org/aquastat/statistics/query/index.html.

41. Hanasaki, N., Yoshikawa, S., Pokhrel, Y. & Kanae, S. A global hydrological simulation to specify the sources of water used by humans. *Hydrol. Earth Syst. Sci.* **22**, 789–817 (2018).

42. Shirakawa, N. Global Estimation of Environmental Flow Requirement Based on River Runoff Seasonality. *Proc. Hydraul. Eng.* **49**, 391–396 (2005).

43. King, J., Brown, C. & Sabet, H. A scenario-based holistic approach to environmental flow assessments for rivers. *River Res. Appl.* **19**, 619–639 (2003).

44. Punjabi, B. & Johnson, C. A. The politics of rural–urban water conflict in India: Untapping the power of institutional reform. *World Dev.* **120**, 182–192 (2019).

45. Padowski, J. C. & Gorelick, S. M. Global analysis of urban surface water supply vulnerability. *Environ. Res. Lett.* **9**, 104004 (2014).

46. Scott, C. A., Flores-López, F. & Gastélum, J. R. Appropriation of Río San Juan water by Monterrey City, Mexico: implications for agriculture and basin water sharing. *Paddy Water Environ.* **5**, 253–262 (2007).

47. Celio, M., Scott, C. A. & Giordano, M. Urban–agricultural water appropriation: the Hyderabad, India case. *Geogr. J.* **176**, 39–57 (2010).

48. F *et al.* Drought In Calif. Creates Water Wars Between Farmers, Developers, Residents. *NPR* (2015).

49. Mekonnen, M. M. & Hoekstra, A. Y. A Global Assessment of the Water Footprint of Farm Animal Products. *Ecosystems* **15**, 401–415 (2012).

50. Hutson, S. S. *et al. Estimated Use of Water in the United States in 2000*. *Estimated Use of Water in the United States in 2000* vol. 1268 http://pubs.er.usgs.gov/publication/cir1268 (2004).

51. Schewe, J. *et al.* Multimodel assessment of water scarcity under climate change. *Proc. Natl. Acad. Sci.* **111**, 3245–3250 (2014).

52. Gosling, S. N. & Arnell, N. W. A global assessment of the impact of climate change on water scarcity. *Clim. Change* **134**, 371–385 (2016).

53. DeAngelis, A. *et al.* Evidence of enhanced precipitation due to irrigation over the Great Plains of the United States. *J. Geophys. Res. Atmospheres* **115**, (2010).

54. Xia, W., Wang, Y. & Wang, B. Decreasing Dust Over the Middle East Partly Caused by Irrigation Expansion. *Earths Future* **10**, e2021EF002252 (2022).

55. Douglas, E. M., Beltrán-Przekurat, A., Niyogi, D., Pielke, R. A. & Vörösmarty, C. J. The impact of agricultural intensification and irrigation on land–atmosphere interactions and Indian monsoon precipitation — A mesoscale modeling perspective. *Glob. Planet. Change* **67**, 117–128 (2009).

56. Condon, L. E. & Maxwell, R. M. Simulating the sensitivity of evapotranspiration and streamflow to large-scale groundwater depletion. *Sci. Adv.* **5**, eaav4574.

57. Seo, S. B., Mahinthakumar, G., Sankarasubramanian, A. & Kumar, M. Conjunctive Management of Surface Water and Groundwater Resources under Drought Conditions Using a Fully Coupled Hydrological Model. *J. Water Resour. Plan. Manag.* **144**, 04018060 (2018).

58. Alcamo, J., Henrichs, T. & Rosch, T. *World Water in 2025 – Global modeling and scenario analysis for the World Commission on Water for the 21st Century*. https://web.archive.org/web/20070613043132/https://www.usf.uni-kassel.de/ftp/dokumente/kwws/kwws.2.pdf (2000).

59. Hanasaki, N. *et al.* An integrated model for the assessment of global water resources – Part 2: Applications and assessments. *Hydrol. Earth Syst. Sci.* **12**, 1027–1037 (2008).

60. Liu, X. *et al.* Environmental flow requirements largely reshape global surface water scarcity assessment. *Environ. Res. Lett.* **16**, 104029 (2021).

61. Faralli, M., Matthews, J. & Lawson, T. Exploiting natural variation and genetic manipulation of stomatal conductance for crop improvement. *Curr. Opin. Plant Biol.* **49**, 1–7 (2019).

62. Gonzalez-Dugo, M. P. *et al.* A comparison of operational remote sensing-based models for estimating crop evapotranspiration. *Agric. For. Meteorol.* **149**, 1843–1853 (2009).

63. Gimpel, J. G., Lovin, N., Moy, B. & Reeves, A. The Urban–Rural Gulf in American Political Behavior. *Polit. Behav.* **42**, 1343–1368 (2020).

64. McDonald, R. I. *et al.* Urban growth, climate change, and freshwater availability. *Proc. Natl. Acad. Sci.* **108**, 6312–6317 (2011).

65. Blanc, E. *et al.* Modeling U.S. water resources under climate change. *Earths Future* **2**, 197–224 (2014).

66. Srinivasan, V., Seto, K. C., Emerson, R. & Gorelick, S. M. The impact of urbanization on water vulnerability: A coupled human–environment system approach for Chennai, India. *Glob. Environ. Change* **23**, 229–239 (2013).